JOURNAL OF MATERIALS SCIENCE **34** (1999) 1009–1015

Wear of 3Y–TZP containing compressive residual stresses at the surface

S. CONOCI, C. MELANDRI, G. DE PORTU
CNR - Research Institute for Ceramic Technology (IRTEC), 48018 Faenza, Italy
E-mail: deportu@irtecl.irtec.bo.cnr.it

Tetragonal zirconia polycrystals doped with 3 mol % yttria (3Y–TZP) was heat treated to stimulate the tetragonal to monoclinic phase transformation in order to induce compressive residual stresses at the surface. Pin-on-disc wear tests were performed at different sliding speeds to evaluate the wear behavior of treated and untreated materials. The friction coefficients were also measured. The conditions for mild and severe wear were defined. The material containing compressive residual stresses had lower wear resistance. A possible explanation for this behavior is discussed.

1. Introduction

Since 1983, when for the first time a large part of the Conference on Wear of Materials [1] was dedicated to ceramics, several studies have been carried out on the wear of ceramics and their practical applications. Nevertheless, reliable and complete data on the wear and friction of many ceramics are still not available. This is mainly due to the fact that wear resistance is not an intrinsic property of materials but the result of an interaction between two or more bodies and depends also on the method used for assessing this parameter.

The potentially high wear resistance of ceramics can be used not only in high performance systems but also in many conventional applications. The development of tough ceramics, like zirconia, has stimulated a particular interest in the basic understanding of wear for this class of materials. These ceramics show considerable mechanical properties, especially toughness, and can be designed to stimulate controlled residual stresses for improving performance. These stresses can be distributed over the whole material; however, surface residual stresses can control the fracture behavior in many cases.

The surface transformation technique [2] in general, generates surface residual compressive stress in a thin layer of material (10–30 μm) and, consequently, has little effect on the properties controlled by large defects. However, the performance of wear-resistant materials is related to the properties of thin surface layers [3]. The basic idea is that the development of a compressive residual stress at the surface of tetragonal zirconia polycrystals doped with 3 mol % yttria (3Y–TZP) increases the apparent surface toughness of the material and, therefore, the resistance to contact damage.

The question is: can this improvement in contact damage affect the wear resistance of this type of zirconia? The aim of this work was to provide an answer to this question for the system studied.

2. Experimental procedure

Discs with a diameter of about 30 mm and a thickness of about 2 mm were prepared by sintering 3 mol % Y_2O_3 containing ZrO_2 (3Y–TZP powder, Tosoh, Japan). The powder was uniaxially pressed at 39 MPa in a steel die and then isostatically cold-pressed at 294 MPa. The samples obtained were sintered in air at 1500 °C for 1 h. The density was measured using Archimede's method and reached the theoretical value of 6.05 g cm^{-3}. The discs were ground by a diamond wheel and polished with 1 μm diamond paste to remove the residual stress induced by grinding. The roughness was assessed by measuring the R_a parameter ($R_a = 0.01$ μm), using a conventional stylus-type instrument (Form Talysurf Plus, Taylor-Hobson, UK). X-ray diffraction analysis (XRD) showed only the presence of the tetragonal (t) phase. In order to stimulate the surface residual stresses the approach suggested by Green [2] was used. The method implies that the samples of Y–TZP are heat treated in an unstabilized ZrO_2 powder bed. In this condition the Y_2O_3 stabilizer can diffuse from the surface into the powder leaving a region, with a reduced amount of stabilizer, in which the transformation during cooling is favored. In our case a thermal treatment at 1420 °C for 36 h was used. The XRD analysis (X-Ray diffractometer, Rigaku Geigerflex, Rigaku, Japan) performed after this procedure showed the presence of about 30% of the monoclinic phase. In order to evaluate the thickness of the transformed layer, a few microns of material were removed in several steps by polishing. After each step the amount of monoclinic phase was assessed by XRD. The surfaces of the material before and after the thermal treatment were observed by optical and scanning electron (SEM) microscopes (Leitz DM RME, Leica AG, Switzerland and Cambridge S 460, Cambridge, UK, respectively).

The toughness (K_{IC}) of both treated and untreated materials as well as the presence of residual stresses and their effect on surface crack propagation were determined by using the indentation technique [4]. A Vickers

TABLE I Physical, mechanical and microstructural parameters of the pin and the discs of different materials

	Pin	Disc	
	WC	3Y–TZP untreated	3Y–TZP treated
Density ($g\,cm^{-3}$)	14.75	6.05	6.05
Grain size (μm)	1–3	0.23 ± 0.02	0.51 ± 0.02
Roughness (μm)	—	0.01	0.01
Hardness (GPa)	14	12.9 ± 0.1	12.1 ± 0.1
K_{IC} ($MPa\,m^{1/2}$)	—	4.0 ± 0.1	6.2 ± 0.5
Thermal Conductivity ($W\,m^{-1}\,K^{-1}$)	121	1.8	—

indenter with loads ranging from 29.4 to 612.5 N was used to stimulate the formation of cracks of different lengths. This procedure was followed after each step to verify the effect of the different amount of monoclinic phase on the residual stress and crack propagation. The amount of residual stress present at different depths of the transformed layer was determined from the relative percentage of the monoclinic phase [5].

Wear tests were carried out in air on both treated and untreated samples using a tribometer (Watzau, Berlin) with an inverted pin-on-disc configuration. Cobalt-bonded tungsten carbide (WC–6% Co) was used as the pin. It had a length of 16 mm, a diameter of 5.64 mm and a radius of curvature of 2.82 mm. Some physical, mechanical and microstructural parameters of the pin and the disks (both treated and untreated samples) are reported in Table I. The force (10 N) and the sliding distance (1 km) were kept constant while different sliding speeds ($v = 0.01, 0.05, 0.1, 0.2, 0.3, 0.4$ and $0.5\ m\,s^{-1}$) were used. Several parameters such as total wear, torque and normal force were continuously recorded via a computer during the test.

The specific wear rate (unit of mass lost per unit of distance and of applied load) was estimated by the weight difference before and after the tests. The specimens were weighed with an analytical balance and the mass lost during each test was measured to an accuracy of (0.01 mg). The friction coefficient was calculated from the torque data using the following expression

$$\mu = \frac{M}{rF} \tag{1}$$

Where M is the torque, r is the radius of the circumference covered by the pin and F is the applied force.

The worn surfaces were observed by SEM and analysed by XRD. The depth and the profile of the worn tracks were assessed by the same instrument used for measuring the roughness. Before the wear tests the discs and the pin were cleaned with acetone in an ultrasonic bath for 10 min, dried at 70 °C for 15 min and cooled at room temperature for 1 h. All wear tests were carried out in air under controlled temperature and humidity (21 °C and 60%, respectively).

3. Results and discussion

Photographs of the surface of the material before and after the thermal treatment are shown in Fig. 1a and b, respectively. The effect of the phase transformation is evident, especially when the Normarski technique is used.

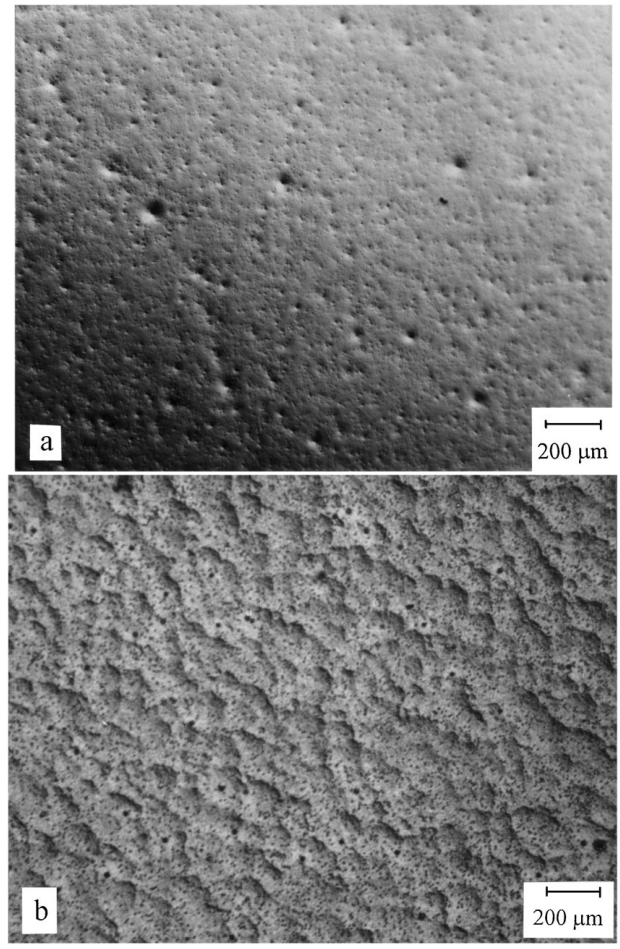

Figure 1 Optical micrographs (Nomarski interference) of the surface of untreated (a) and treated (b) samples.

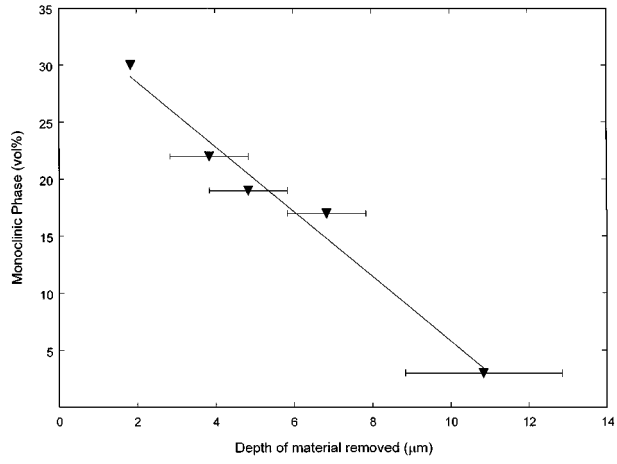

Figure 2 Percentage of the monoclinic phase as a function of the depth of material removed for the thermal-treated material.

The percentage of monoclinic phase (m), transformed after the thermal treatments, for each step, was evaluated by XRD analysis taking into account the scattering factor for each phase [6]. The results are plotted as a function of the depth of the removed material in Fig. 2. It appears that the amount of monoclinic phase decreases linearly from the surface to a depth of about 12 μm.

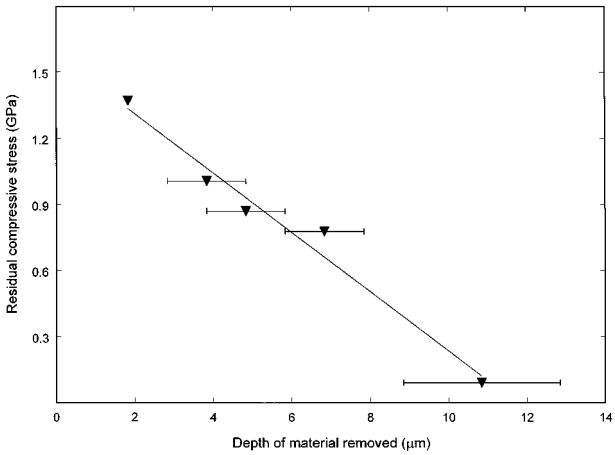

Figure 3 Value of the residual surface compressive stress as a function of the depth of material removed for the thermal-treated material.

The residual compressive stress profile present inside the transformed layer was evaluated taking into account the percentage of monoclinic phase at different depths, using the following equation [5]

$$\sigma_c \cong \frac{1}{3}\left(\frac{\Delta V}{V}\right)\frac{E V_i}{1-\nu} \qquad (2)$$

where $\Delta V/V = 0.049$ is the fractional molar volume increase due to the tetragonal-to-monoclinic transformation [7], V_i is the volume fraction of monoclinic phase, E is the Young's modulus (210 GPa) and ν is the Poisson's ratio (0.25) [8]. The calculated values of σ_c as a function of the depth of the removed material are plotted in Fig. 3.

The presence of a residual stress at the surface has been revealed also by the indentation technique. The cracks starting from a Vickers impression on untreated (stress-free) samples (Fig. 4a) are longer than those starting from an impression produced with the same load on the surface of heat-treated (stressed) samples (Fig. 4b). Using the crack length data, the toughness calculated according to Anstis *et al*. [4] is $K_{IC} = 4.0 \pm 0.1$ MPa m$^{1/2}$ and $K_{IC} = 6.2 \pm 0.5$ MPa m$^{1/2}$ for untreated and treated materials, respectively. These results reveal that the phase transformation induced by thermal treatment improves the surface toughness by ∼50%. The values of K_{IC} as well as the measurements of crack length as a function of indentation load suggest that the material containing compressive residual stresses at the surface exhibits superior resistance to static contact damage. Detailed information on this subject can be found elsewhere [9].

Unfortunately, as can be seen from Fig. 5, a resistance to static contact damage does not necessarily lead to an improvement of wear resistance to sliding contact. Fig. 5 shows the values of specific wear as a function of sliding speed for both stress-free and stressed materials. It is evident that the material containing surface compressive residual stress has lower resistance to sliding wear than the stress-free material. A more in-depth evaluation of the data suggests that the wear process can be divided into two regions: mild wear and severe wear. The reasons for such behavior and the high values

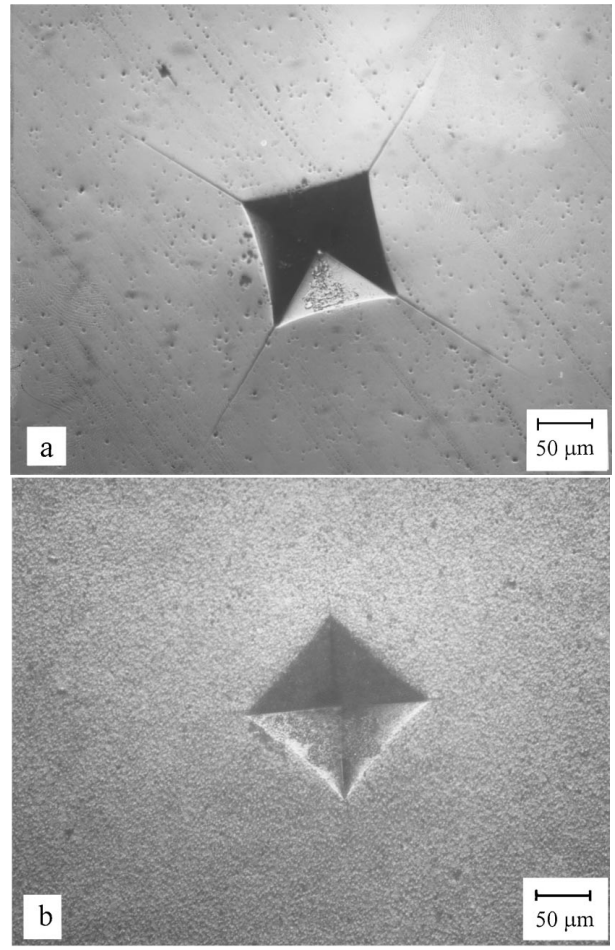

Figure 4 Artificial cracks on (a) untransformed and (b) transformed surfaces, obtained using a Vickers indenter with a load of 20 kg.

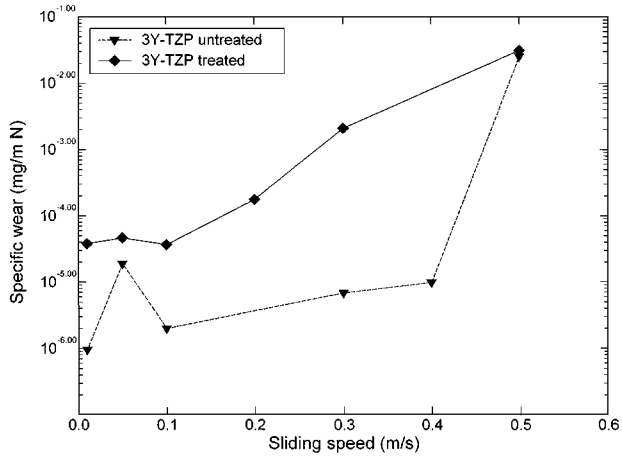

Figure 5 Specific wear as a function of sliding speed for transformed and untransformed material.

of the friction coefficient of the two different materials can be interpreted as follows.

3.1. Mild wear

For the stress-free material, strong grain boundaries can prevent the formation of large cracks at sliding speeds lower than 0.4 m s^{-1}. In this case the stress concentration at grain boundaries is not sufficient to stimulate a large t → m transformation but can enhance the plastic deformation before crack nucleation and growth (Fig. 6).

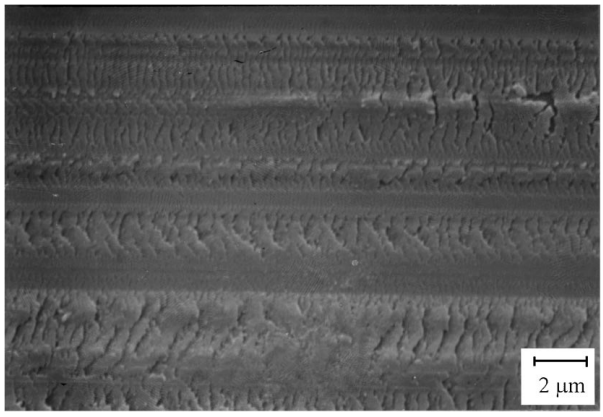

Figure 6 SEM micrograph of the worn surface (sliding speed = 0.03 m s^{-1}) of an untreated sample. Plastic deformation is visible.

The peak in the specific wear observed at a sliding speed of 0.05 m s^{-1} can be attributed to a possible exaggerated phase transformation due to the experimental conditions. In fact, it has been shown [10, 11] that 3Y–TZP undergoes an enhanced t $\rightarrow$ m phase transformation at about 200–300 °C especially in a humid environment. It is possible that at $v = 0.05$ m s^{-1} the temperature at the contact point reaches a value similar to that mentioned above, leading to a catastrophic transformation with the contribution of a relative high humidity value (60%). In this condition the wear mechanism becomes similar to that observed for the stressed material.

For the stressed material the presence at the surface of $\sim$30% of monoclinic phase leads to the formation of microcracking around monoclinic particles. In addition, the procedures for stimulating residual stresses induced the grain growth of the remaining tetragonal particles ($\sim$0.5 μm) so that they became closer to the critical size. In this situation the energy necessary to transform these particles into monoclinic is very low. This means that a large number of grains undergo the t $\rightarrow$ m transformation, leading to extensive surface cracking (Fig. 7) with a consequent production of large pits (Fig. 8a and b) and hence a lower wear resistance. Single grains can also be loosened during rubbing, and because monoclinic grains are softer than the tetragonal

Figure 7 SEM micrograph of the worn surface (sliding speed = 0.01 m s^{-1}) of a treated sample. Magnification of a pit-free area. Extensive surface cracking is visible.

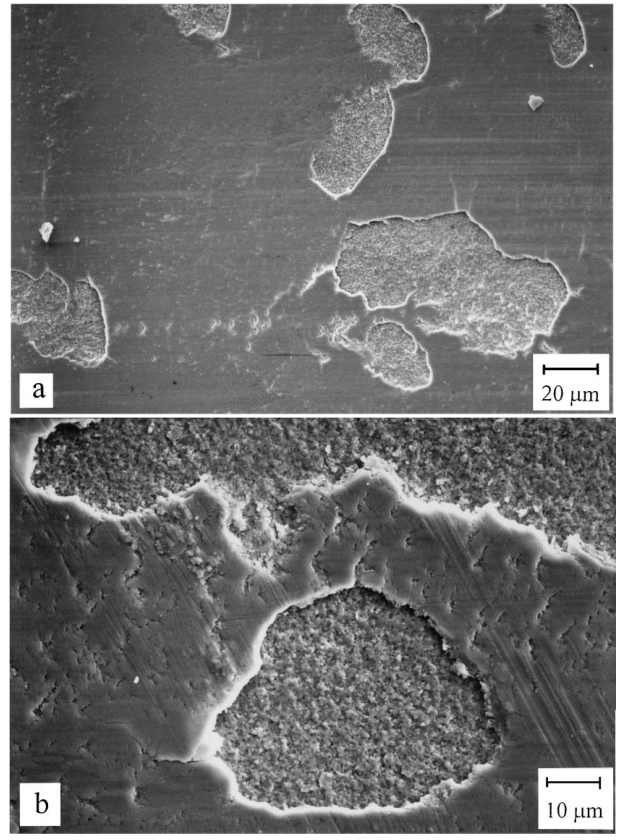

Figure 8 Tipical pits observed in the worn surface of a thermal-treated sample. Sliding speed: (a) 0.05 m s^{-1} and (b) 0.01 m s^{-1}.

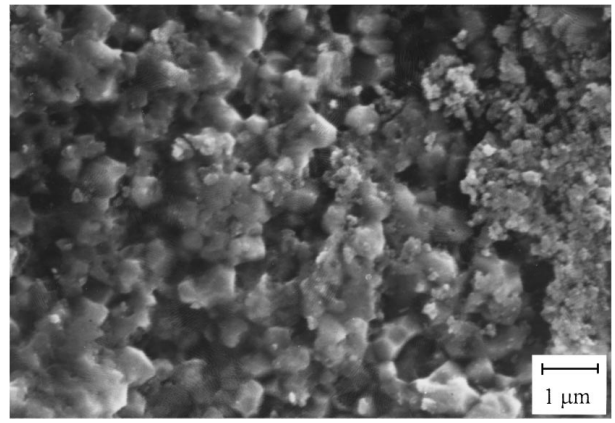

Figure 9 Magnification of the surface inside the pits of treated material (sliding speed = 0.01 m s^{-1}). Intergranular fracture is evident. Powder of crushed grains is also visible.

ones they can be crushed, forming small particles that can be smeared on the surface in some part of the track (Fig. 9).

3.2. Severe wear

Increasing the sliding speed from 0.4 m s^{-1} to 0.5 m s^{-1} causes a significant increase in the specific wear of the stress-free material. This could be due to the high plastic deformation as a consequence of the high temperatures reached at the contact (Fig. 10). In this situation grains or groups of grains initially loosened from the surface due to the t $\rightarrow$ m transformation are smeared on the surface and form flakes (Fig. 11). As a consequence of such a mechanism a layer of surface material is formed. Fatigue processes and thermal

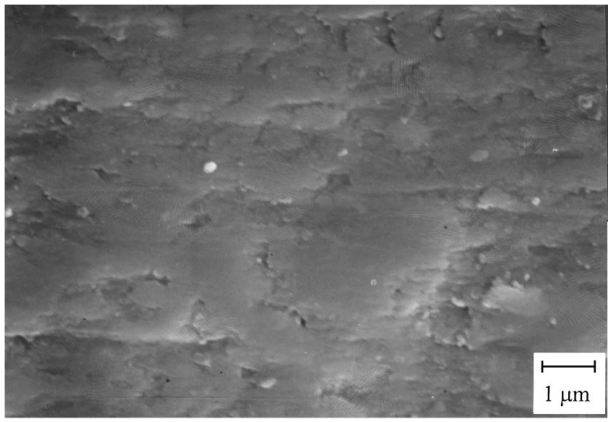

Figure 10 Magnification of smeared and plastically deformed layer in the worn surface (sliding speed = 0.5 m s^{-1}) of untreated material.

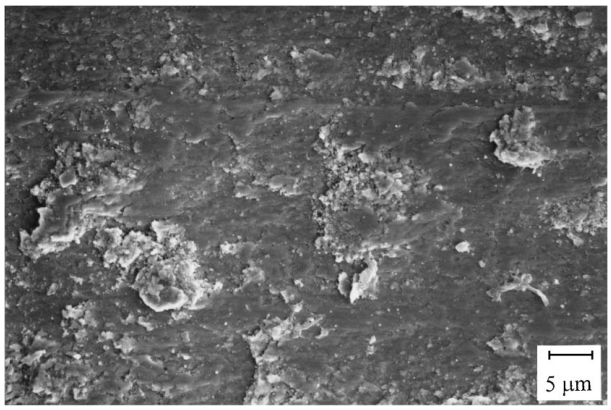

Figure 11 Flakes of material smeared at the surface of untreated sample (sliding speed = 0.5 m s^{-1}).

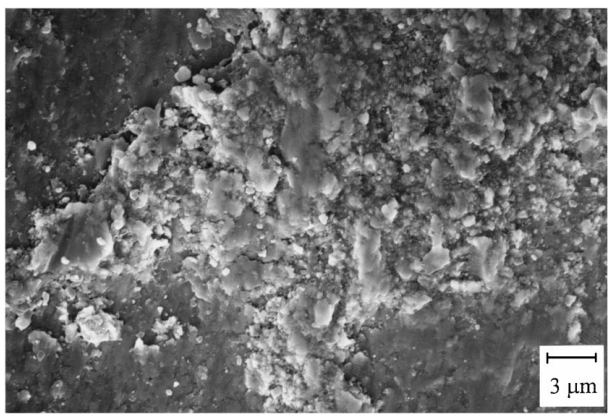

Figure 12 Crushed material detached from the surface on an untreated sample (sliding speed = 0.5 m s^{-1}).

cycling can crack this layer and detach large parts of material from the surface (Fig. 12).

For the stressed material the change from mild to severe wear is not so sharp as in the stress-free samples. This behavior may result from the fact that the mechanism of mild wear is still present together with mechanisms stimulated by residual stresses and/or related to plastic deformation.

During rubbing at sliding speeds greater than 0.1 m s^{-1} the temperature at the contact point could be so high as to re-transform the monoclinic phase into tetragonal with an appreciable volume reduction.

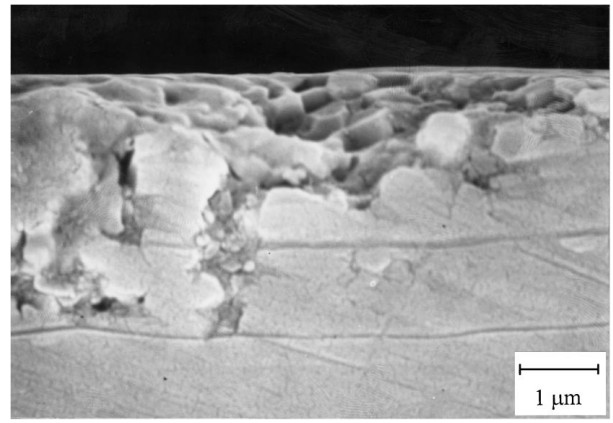

Figure 13 Cracks parallel to the surface, underneath the worn groove of transformed material.

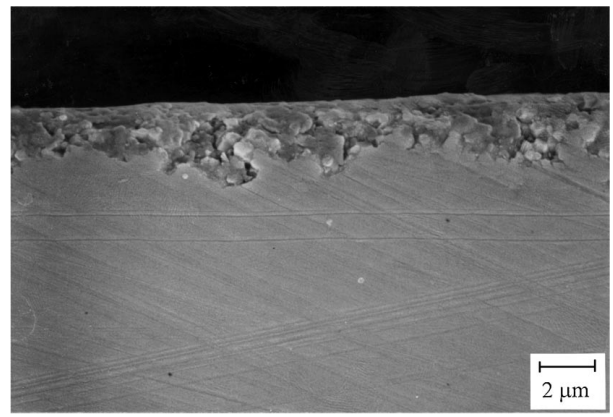

Figure 14 Cracks parallel to the surface, far from the worn groove of transformed material.

This transformation produces a change in the sign of the stresses, i.e. from compressive to tensile stresses, at the boundary between the thin surface layer and the bulk. As the results of the discontinuity in the stresses, wear particles may be formed by crack formation and propagation.

In addition, cracks parallel to the surface were observed (Fig. 13) in the cross-section of the material at the depth of about 5–7 μm. These cracks were present in the whole sample, also quite far from the worn surface (Fig. 14). Because these cracks were not observed in the stressfree material, they can be attributed to the very high compressive stresses measured at the surface.

When the crack reaches this depth the material can be easily removed and the wear continues to increase, even if the other mechanisms, as mentioned above, are no longer active. At a sliding speed above 0.3 m s^{-1} the depth of the track is about 250 μm and the effect of the surface layer is negligible. The value of specific wear is therefore very similar to that observed for the highest speed of the stress-free material, and the wear mechanism is similar for both materials (Figs 11, 12, 15 and 16).

3.3. Friction

The friction coefficients as a function of sliding speed for both materials are plotted in Fig. 17. The analysis of the data suggests the following possible explanation.

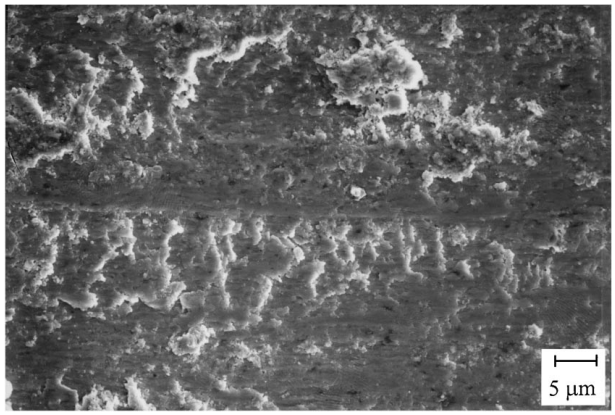

Figure 15 Micrograph of the worn surface (severe wear) of treated material. Flakes of smeared grains and plastic deformation are visible.

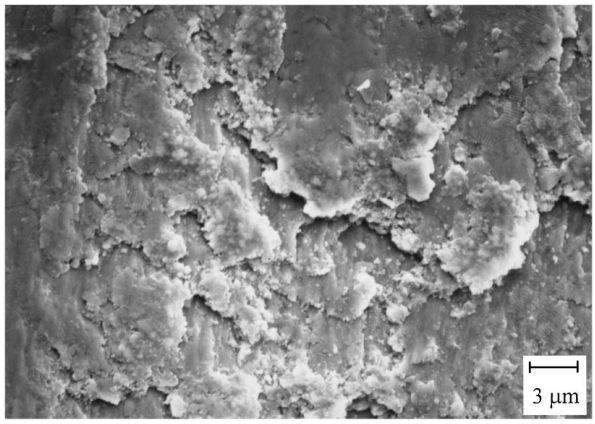

Figure 16 Flakes of smeared material in the groove of the worn surface of treated sample.

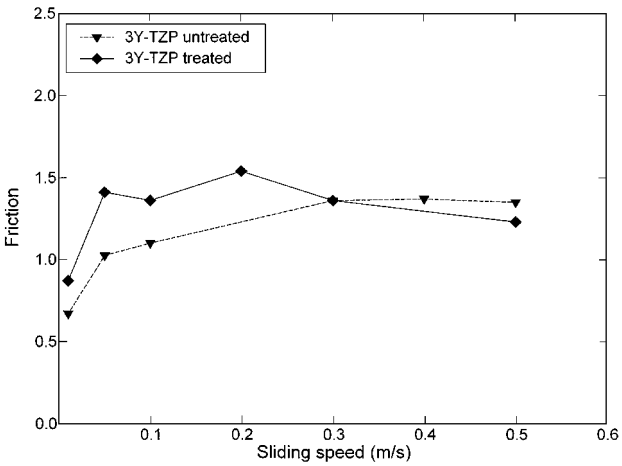

Figure 17 Friction coefficient as a function of sliding speed for treated and untreated material.

In the case of the stress-free material, the friction coefficient is always very high but is independent of the wear rate. It increases steadily and reaches a plateau at a sliding speed of 0.3 $m\,s^{-1}$. This increase can be attributed to a change in viscosity of the thin layer of plastically deformed grains smeared at the surface with an increase in temperature at the contact point. The use of a pin harder than 3Y–TZP can increase the plastic deformation of material that is prone to this behavior.

According to Rice [12] the plastic deformation may result in an increase in friction. In addition, for the stress-free samples the relatively smooth sliding surface can lead to an increase of the cohesive force between the two contact surfaces due to the reduction of the absorbed air film, similar to vacuum conditions [13].

The friction coefficient of the stressed material is higher than that of the stress-free material except at sliding speeds higher than 0.3 $m\,s^{-1}$. In the latter case, as described above, the wear mechanisms are similar for both materials and hence the friction coefficients are also similar. Below this sliding speed, as soon as it exceeds 0.01 $m\,s^{-1}$ the removal of materials by pull-out of grains or fracture in microcracked regions (large pits) generates a rough surface. As a result, the friction increases considerably, favoring the occurrence of wear particles in the contact area.

4. Conclusions

The stimulation of compressive surface residual stresses by phase transformation in 3Y–TZP improves the contact damage resistance considerably. The apparent surface toughness increases by more than 50% (from 4.0 $\pm$ 0.1 MPa $m^{1/2}$ to 6.1 $\pm$ 0.5 MPa $m^{1/2}$). Nevertheless, the presence of microcracking associated with the t $\rightarrow$ m transformation, the increase of the size of tetragonal grains (due to the thermal treatment) and the weakness of the monoclinic phase reduce the wear resistance of this material.

The friction is very high and can be due to two different mechanisms in mild and severe wear regions. In the first case it can be caused by the loosening of microcracked regions by spalling of individuals grains or large pits, with a consequent roughening effect. In the latter case the high friction coefficient can be attributed to the observed plastic deformation, favored by possible high flash temperature, and the large contact area due to the penetration of the pin in the zirconia discs ($\sim$250 μm at the higher sliding speed).

At the highest sliding speed the wear and friction are very similar for both stressed and stress-free material, indicating a similar wear mechanism.

Acknowledgements

The authors are grateful to Eniricerche for providing the fellowship for S. Conoci on behalf of the Italian Ministry of University and Scientific Research.

References

1. Proceedings of the International Conference on Wear of Materials, Reson, VA, 1983, edited by V. D. Fréchette, W. C. LaCourse and V. L. Burdick (American Society of Mechanical Engineers, New York, 1983).
2. D. J. GREEN, *J. Am. Ceram. Soc.* **66** (1983) C-78.
3. I. M. HUTCHINGS, in "Tribology: Friction and Wear of Engineering Materials" (Edward Arnold Publ., London, 1992).
4. G. R. ANSTIS, P. CHANTIKUL, B. R. LAWN and D. B. MARSHALL, *J. Am. Ceram. Soc.* **64** (1981) 533.
5. D. J. GREEN, F. F. LANGE and M. R. JAMES, *ibid.* **66** (1983) 623.

6. H. P. KLUG and L. E. ALEXANDER, in "X-Ray Diffraction Procedures for Polycrystalline and Amorphous Materials" (2nd Edn., J. Wiley & Sons, New York, 1974).
7. A. V. VIRKAR, J. L. HUANG and R. A. CUTLER, *J. Am. Ceram. Soc*. **70** (1987) 164.
8. D. J. GREEN, R. H. J. HANNINK and M. V. SWAIN, in "Transformation Toughening of Ceramics" (CRC Press, Boca Raton, FL, 1989).
9. G. DE PORTU and S. CONOCI, in print in the *J. Am. Ceram.* Soc. **80** (1997) 3242.
10. M. MATSUI, T. SOMA and I. ODA, in "Science and Technology of Zirconia II, Advances in Ceramics, Vol. 12," edited by N. Claussen, M. Ruhle and A. H. Heuer (American Ceramic Society, Columbus, OH, 1984) p. 371.
11. M. WATANABE, S. IIO and I. FUKUURA, *ibid*., p. 391.
12. R. W. RICE, *Ceramic Engineering and Science Proceedings* **6** (1985) 940.
13. S. SASAKI, *Wear* **134** (1989) 185.

Received 23 November 1997
and accepted 18 August 1998